SOME RESULTS OF STELLARATOR OPTIMIZATION

M.I.Mikhailov[1], W.A.Cooper[2], M.F.Heyn[3], M.Yu.Isaev[1], A.A.Ivanov[4], V.N.Kalyuzhnyj[5], S.V.Kasilov[5], W.Kernbichler[3], A.A.Martynov[4], S.Yu.Medvedev[4], V.V.Nemov[5], J.Nührenberg[6], Yu.Yu.Poshekhonov[4], M.A.Samitov[1], V.D.Shafranov[1], A.A.Skovoroda[1], A.A.Subbotin[1], R.Zille[6]

[1] Russian Research Centre "Kurchatov Institute", Moscow, Russia
[2] CRPP, Association Euratom-Confédération Suisse, EPFL, Lausanne, Switzerland
[3] Institut für Theoretische Physik, Technische Universität Graz, Graz, Austria
[4] Keldysh Institute, Russian Academy of Science, Moscow, Russia
[5] IPP, NSC "Kharkov Institute of Physics and Technology", Kharkov, Ukraine
[6] Max-Planck-Institut für Plasmaphysik, IPP-EURATOM Association, Germany

Abstract

The collisionless confinement of all reflected particles with orbits that start within the inner half of the plasma of a stellarator with poloidal direction of the contours of the magnetic field strength B is shown computationally to be possible. It is also demonstrated that the confinement achieved is well compatible with the fulfilment of Mercier stability criterion.

1. Introduction

One of the possible ways to improve the plasma confinement in stellarators is to "restore" the symmetry of the particle drift motion equations. This restoration implies the magnetic field strength $B = |\mathbf{B}|$ to be a twodimensional function in the magnetic (Boozer) flux coordinates s, θ_B, ζ_B [1]. The possibility of such quasisymmetry, helical [2], $B = B(s, \theta_B - \zeta_B)$, or axial [3], $B = B(s, \theta_B)$, is now widely used in stellarator optimization.

For the third possible direction of lines B=constant on the magnetic surfaces, the poloidal onefor which $B = B(s, \zeta_B)$, the condition of quasisymmetry can not be fulfilled, particularly not in a linear approximation with respect to the distance from the magnetic axis. Taking in mind that for the configuration without net toroidal current the fulfilment of the condition $B = B(s, \zeta_B)$ leads to the ideal *isodynamic* case, in which there are no secondary currents and the particle drift orbits lie on the magnetic surface, one can suggest that some less restrictive conditions which can be satisfied could still lead to significant improvement of the particle confinement. For such type of the stellarators the condition of *quasi-isodynamicity* (*qi*) was suggested in Ref.[4]. This condition requires the "banana" centers of deeply to moderately deeply trapped particles to move along the magnetic surface. That means that for these particles the configuration is omnigenous [5]. The barely reflected particles have a "diffusive-like" behavior of the collisionless drift motion and are eventually lost. It occurs, nevertheless, that for power plant parameters the α-particles born within the inner quarter of the plasma column are confined longer than the energy slowing down time. Thus, there are at least two different mechanisms to confine for sufficiently long time the collisionless reflected particles orbits. The ratio of the numbers of particles in these two groups may be different. As a limiting case one can try to find configurations in which there is only one group of particles, those reflected within the periods.

This limiting case is considered in the present paper. Therefore, the possibility to fulfil the *qi* condition for all reflected particles is studied below analytically and numerically. Some results of these investigations were presented earlier in Refs. [6-8]. In the next Section the analytical considerations in near-axis approximation are presented with respect to possibility to fulfil the *qi* condition for all reflected particles. The third Section describes the results of a numerical optimization and is followed by conclusions.

2. Analytical investigation of quasi-isodynamicity condition

In order to fulfil the *qi* (or omnigeneity) condition for all reflected particles one needs to satisfy the condition of pseudosymmetry [9]. For the configurations considered here with poloidal

direction of the B contours this condition requires B to be a two-dimensional function of flux coordinates (not necessarily the magnetic ones) with straight magnetic field lines, $B = B(s, \zeta)$. For a net-current free configuration the magnetic field can be expressed in these coordinates as follows:

$$\mathbf{B} = F\nabla\zeta + \nabla\varphi - \nu\nabla s = \nabla\Psi \times \nabla\zeta + \nabla\Phi \times \nabla\theta. \quad (1)$$

with F, Ψ, Φ the poloidal current, the poloidal flux and the toroidal flux, respectively.

Using the relations

$$B^2 = B^i B_i = \frac{F\Phi'}{\sqrt{g}}(1+\frac{1}{F}\frac{\partial\varphi}{\partial\zeta}|_{\mathbf{B}}), \quad dl = \frac{B\sqrt{g}}{\Phi'}d\zeta, \quad (2)$$

it is easy to find the expression for the second adiabatic invariant:

$$\mathcal{J} = \int V_{||}dl = \int \frac{V_{||}F}{B}(1 + \frac{1}{F}\frac{\partial\varphi}{\partial\zeta}|_{\mathbf{B}})d\zeta$$

$$\propto \int \frac{\sqrt{B_{reflect} - B}}{B}F(1 + \frac{1}{F}\frac{\partial\varphi}{\partial\zeta}|_{\mathbf{B}})d\zeta. \quad (3)$$

Here $\frac{\partial\varphi}{\partial\zeta}|_{\mathbf{B}} = \frac{\partial\varphi}{\partial\zeta} + \iota\frac{\partial\varphi}{\partial\theta}$, $\sqrt{g} = (\nabla s \cdot [\nabla\theta \times \nabla\zeta])^{-1}$.

Below it is suggested that $\zeta = 0$ corresponds to minimum of B and $\zeta = \pm\pi$ correspond to maximum of B. For the usually considered case of "stellarator symmetry" in near-axis approximation the function φ can be expressed in the form

$$\varphi = \sum_n \varphi_n \sin(\theta + n\zeta) = A_1 \sin\theta + A_2 \cos\theta,$$

$$A_1 == \sum_n \varphi_n \cos n\zeta, \quad A_2 = \sum_n \varphi_n \sin n\zeta. \quad (4)$$

By introducing the coordinate $\theta_0 = \theta - \iota\zeta$, which is constant along the magnetic field line, the derivation of φ along the magnetic field line can be presented as

$$\frac{\partial\varphi}{\partial\zeta}|_{\mathbf{B}} = \sin\theta_0(A_1\cos\iota\zeta - A_2\sin\iota\zeta)' +$$

$$+\cos\theta_0(A_1\sin\iota\zeta + A_2\cos\iota\zeta)' \quad (5)$$

where $'$ denotes the derivative with respect to ζ. The omigeneity condition requires the even part of $\frac{\partial\varphi}{\partial\zeta}|_{\mathbf{B}}$ to be zero, so that

$$A_1\sin\iota\zeta + A_2\cos\iota\zeta = 0. \quad (6)$$

It is easy to see that exact fulfilment of this condition is not possible for finite ι (see, also, Ref.[10]).

The radial dependence of $\mathcal{J}$ permits one to has closed contours of $\mathcal{J}$ inside the plasma even if the condition (6) is not satisfied exactly. A simple test was made to estimate the possible accuracy of the fulfilment of this condition. The minimization of the integral

$$\int_{-\pi}^{\pi}(A_1\sin\iota\zeta + A_2\cos\iota\zeta)^2 d\zeta \quad (7)$$

with respect to φ_n with the condition $A_1(0) = 1$ shows that for $-6 \le n \le 6$ the accuracy of the fulfilment of the condition (6) is of the order of 10^{-5} and the periodic function $A_1(\zeta)$ goes to zero for $\zeta = \pm\pi$. Fig.1 shows the function $A_1(\zeta)$ on the period and the contours of B in Boozer coordinates for this nearly omnigenous configuration. It is seen that the B contours have a cosine-like behavior. The positions of the extrema move along the magnetic field lines and the amplitude gradually disappear with approaching $\zeta = \pm\pi$.

3. Results of the numerical optimization

The optimization procedure was performed with the VMEC code [11] for the equilibrium computation and the JMC code [12] for obtaining the spectrum of B in magnetic coordinates. The orbit integration code in magnetic coordinates [13] was used as a diagnostic to evaluate the quality of the optimized configuration. A six-fold period configuration with $< \beta > \approx 5\%$ and aspect ratio $A \approx 12$ is considered.

For the construction of the penalty function the condition of pseudosymmetry was used based on the formulation presented in Ref.[14]. In addition, the requirement of the contours of $\mathcal{J}$ started at the 1/2 of plasma minor radius to be closed inside the plasma column was imposed. At the final stage of the optimization, the condition of the Mercier and resistive mode stability was incorporated, too. Fig. 2 shows the 3D view of the optimized configuration. The field strength B on the boundary magnetic surface is marked by grey intencity. The characteristic feature of the configuration found is near-zero curvature of the magnetic axis in the cross-sections with extremes of the magnetic field on the magnetic axis. It is

seen from Fig. 3 that only small islands in the B contours are left near the maximum of B (the middle of the period). Fig. 4 shows the set of contours of $\mathcal{J}$ for $B_{\text{reflect}} = B_{min} + i\Delta B/8$, $i = 1, ...6$, $\Delta B = (B_{max} - B_{min})/8$, with B_{max}, B_{min} corresponding to extremes of B at 1/2 of the plasma minor radius. One can expect that the closure of these contours guarantees good particle confinement in a major part of the plasma column. The quality of the α-particle confinement was checked by direct calculation of one thousand particles' drift orbits during ten seconds for power-plant dimensions. These calculations have shown that there is no loss of particles started at 1/2 of the minor plasma radius. The history of losses of particles started at 2/3 of plasma minor radius is shown in Fig. 5. Fig. 6 demonstrates the typical orbit of a trapped particle started at 2/3 of plasma radius. Here the color is defined by the value of the parallel particle's velocity. It is seen that the part of the trajectories with the same sign of the parallel velocity corresponds to the external (internal) part of the "banana" trajectory on the outward and to the internal (external) part on the inward part of the plasma column. This may be the reason of the small bootstrap current in such type of configuration (Ref. [15]).

The optimized configuration was investigated by field line following codes, too (see, e.g. Ref. [16]). Fig. 7 shows the radial dependence of the effective ripple determining the level of transport in the $1/\nu$ regime.

The self-consistency of the VMEC equilibrium description was checked by the exact two-dimensional moment of the 3d analog of the Grad-Shafranov equation [17] and solved for the poloidal flux function with the same input plasma profiles. Fig. 8 shows the rotational transform profiles obtained by different codes. It is seen that except the near magnetic axis region all methods give the same results. It provides an additional check of the nested flux surface solution accuracy and in particular an absence of large magnetic islands.

Finally, Fig. 9 shows that the Mercier and resistive modes are stable for $< \beta >= 4.8\%$.

Conclusions It is shown that using $\mathcal{J}$-optimization together with optimization toward pseudosymmetry (i.e using information about the magnetic field strength only, without direct calculation of particle drift motion) permits to find configurations with good collisionless particle confinement for power-plant dimensions. It is shown also that these criteria for confinement improvement are well compatible with the conditions of Mercier and resistive mode stability.

Acknowledgments This work was supported by INTAS Grant No 99-00592, by the Russian-Germany agreement WTZ-RUS-01/581, by the Russian Federal program on support of leading scientific schools, Grant No 00-15-96526, by the Russian Fund for Basic Research, Grant No 00-02-17105, by the Fonds National Suisse de la Recherche Scientifique and Euratom, by the Association EURATOM-OEAW and by the Austrian Academy of Sciences.

References

[1] Boozer A., Phys. Fluids, **26** (1983) 496.

[2] Nührenberg J. and Zille R., Phys. Lett. A **129** (1988) 113.

[3] Nührenberg J., Lotz W., Gori S. Theory of Fusion Plasmas (Varenna 1994), Editrice Compositori, Bologna (1994) 3.

[4] Gori S., Lotz W., Nührenberg J., Theory of Fusion Plasmas (International School of Plasma Physics), Bologna: SIF (1996) 335.

[5] Hall L.S., McNamara B., Phys. Fluids, **18** (1975) 552.

[6] Mikhailov M.I., Isaev M.Yu., Nührenberg J. et. al., 28th EPS Conf. on Controlled Fusion and Plasma Physics, Funchal, Portugal, ECA Vol. **25A** (2001) 757 (http://epsppd.epfl.ch/Madeira/html/authors/nav/AutS08fr.html).

[7] Subbotin A.A, Cooper W.A., Isaev M.Yu. et al., 29th EPS Conf. on Controlled Fusion and Plasma Physics,Montreux, 2002.

[8] Mikhailov M.I., Shafranov V.D., Subbotin A.A. et al., Nucl. Fusion. in print.

[9] Mikhailov M.I., Cooper W.A., Isaev M.Yu., Shafranov V.D., Skovoroda A.A., Subbotin A.A. Theory of Fusion Plasmas (International School of Plasma Physics), Bologna: SIF (1998) 185.

[10] Cary J.R., Shasharina S.G, Phys. Rev. Letters **78** (1997) 674.

[11] Hirshman S.P. and Betancourt O., J. of Comput. Physics **96** (1991) 99.

[12] Nührenberg J., Zille R., Theory of Fusion Plasmas (Varenna 1987), Editrice Compositori, Bologna (1988) 3.

[13] Fowler R.H., Rome J.A., Lyon J.F., Phys. Fluids **28** (1985) 338.

[14] Skovoroda A. A. Plasma Phys. Rep. (1998) **24** 989.

[15] Cooper W.A., S. Ferrando i Margalet, Allfrey S.J., et al., 29th EPS Conf. on Controlled Fusion and Plasma Physics,Montreux, 2002, Invited paper, to be published in Plasma Phys. and Contr. Fusion.

[16] Nemov V.V., Kasilov S.V., Kernbichler W., Heyn M.F., Phys. Plasmas **6** (1999) 4622.

[17] W.A. Cooper, J. Nührenberg, V.V. Drozdov, A.A. Ivanov, A.A. Martynov, S.Yu. Medvedev, Yu.Yu. Poshekhonov, M.Yu. Isaev, M.I. Mikhailov, "3D Equilibrium Averaged Description and Consistency Check"// 29th EPS Conference, Montreux, Switzerland, 2002.

Figure captions

Fig.1. (a): results of test optimization on φ_n. The function $A_1(\zeta)$, optimized to quasi-isodynamicity; (b): the magnetic field lines (straight lines) and contours of B in magnetic coordinates for the set of φ_n determined by minimization of expression (6).

Fig.2. Boundary magnetic surface of the optimized configuration also showing the magnetic topography.

Fig.3. The contours of B on the magnetic surface with $s = 0.25$ for the optimized configuration.

Fig.4. $\mathcal{J}$ contours for increasing values of B_{ref} in polar-coordinate representation $\sqrt{s}, \theta$ with s being the flux label.

Fig.5. Collisionless α-particle confinement in the optimized configuration as a function of the time of flight. Particles are started at $s_{start} = 0.44(2/3$ of the plasma radius).

Fig.6. Typical orbit of collisionless α-particle in optimized configuration in polar representation. The darkness of the line defines the direction and value of the parallel velocity (gray corresponds to positive direction, black means negative direction).

Fig.7. Radial dependence of the "effective ripple" for the optimized configuration.

Fig.8. Radial profiles of the rotational transform from the VMEC (dots) and obtained from 2D description in Riemannian space for two different representation for ι (gray and black lines).

Fig.9. Mercier and resistive modes stability along the radial coordinate.

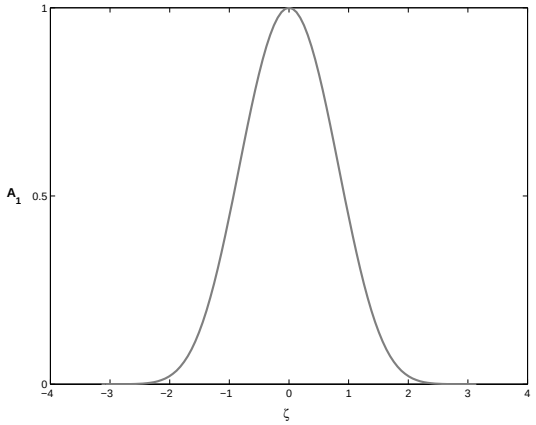

Fig. 1a.

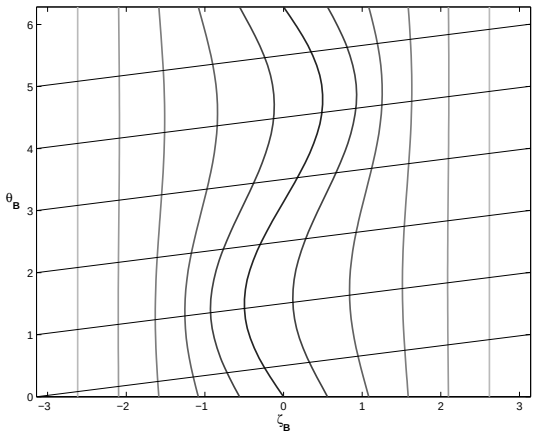

Fig. 1b.

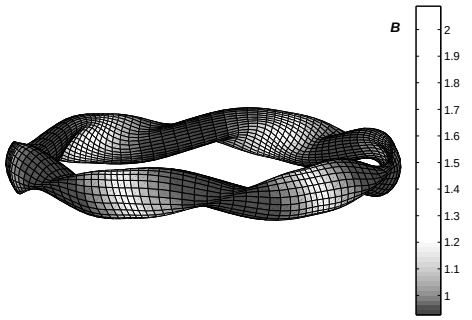

Fig. 2.

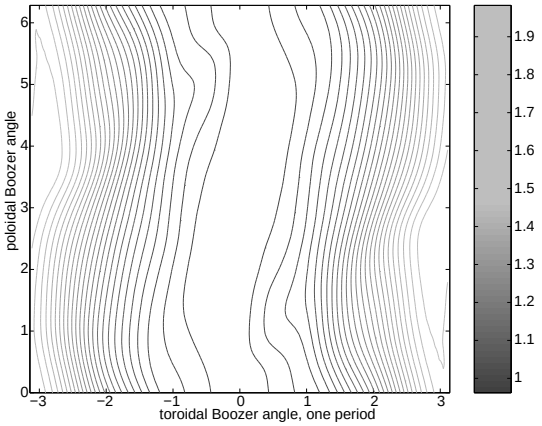

Fig. 3.

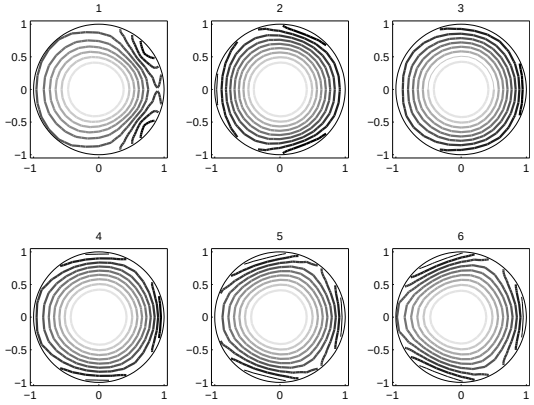

Fig. 4.

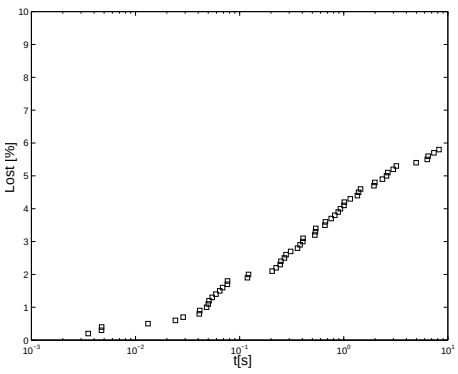

Fig. 5.

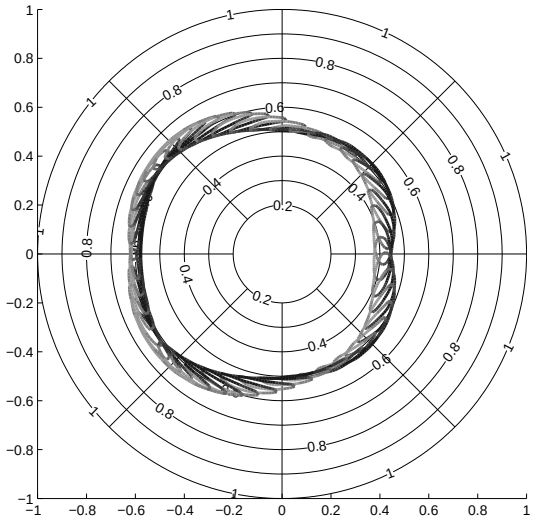

Fig. 6.

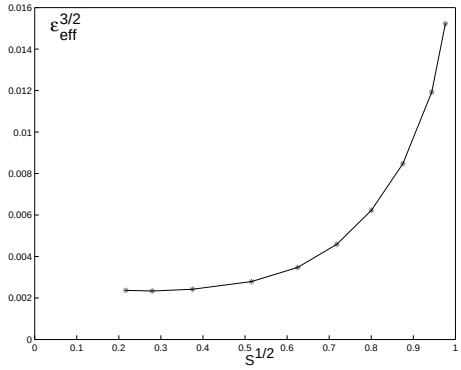

Fig. 7.

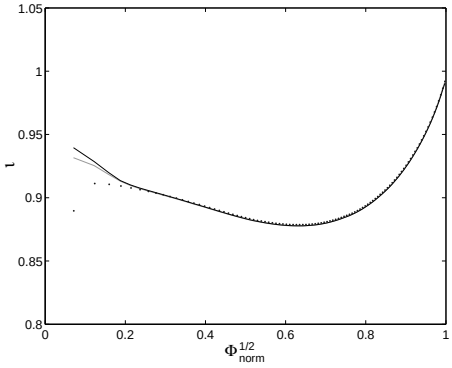

Fig. 8.

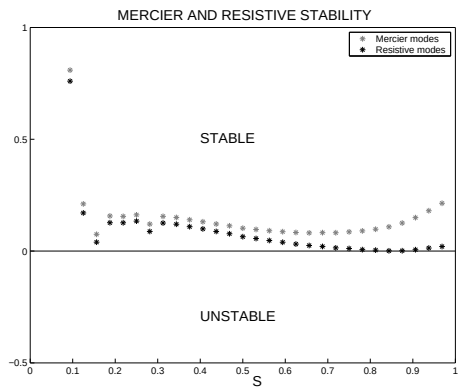

Fig. 9.